Published in final edited form as:
Mol Microbiol. 2012 November ; 86(3): 645–660. doi:10.1111/mmi.12006.

Involvement of WalK (VicK) Phosphatase Activity in Setting WalR (VicR) Response Regulator Phosphorylation Level and Limiting Crosstalk in *Streptococcus pneumoniae* D39 Cells[#]

Kyle J. Wayne[1], **Shuo Li**[1], **Krystyna M. Kazmierczak**, **Ho-Ching T. Tsui**, and **Malcolm E. Winkler**[*]
Department of Biology, Indiana University Bloomington, 1001 East Third Street, Bloomington, Indiana 47405

Abstract

WalRK (YycFG) two-component systems (TCSs) of low-GC Gram-positive bacteria play critical roles in regulating peptidoglycan hydrolase genes involved in cell division and wall stress responses. The WalRK (VicRK) TCSs of *Streptococcus pneumoniae* (pneumococcus) and other *Streptococcus* species show numerous differences with those of other low-GC species. Notably, the pneumococcal WalK sensor kinase is not essential for normal growth in culture, unlike its homologues in *Bacillus* and *Staphylococcus* species. The WalK sensor kinase possesses histidine autokinase activity and mediates dephosphorylation of phosphorylated WalR~P response regulator. To understand the contributions of these two WalK activities to pneumococcal growth, we constructed and characterized a set of *walK* kinase and phosphatase mutants in biochemical reactions and in cells. We identified an amino acid substitution in WalK that significantly reduces phosphatase activity, but not other activities. Comparisons were made between WalRK regulon expression levels and WalR~P amounts in cells determined by Phos-tag SDS-PAGE. Reduction of WalK phosphatase activity resulted in nearly 90% phosphorylation to WalR~P, consistent with the conclusion that WalK phosphatase is strongly active in exponentially growing cells. WalK phosphatase activity was also shown to depend on the WalK PAS domain and to limit crosstalk and the recovery of WalR~P from *walK*$^{+}$ cells.

Keywords

WalR response regulator; WalK sensor kinase; WalK phosphatase activity; pneumococcus; Phos-tag SDS-PAGE

Introduction

The WalRK (YycFG) two-component regulatory system (TCS) plays important roles in maintaining peptidoglycan and surface homeostasis and in responding to cell wall stresses in low-GC Gram-positive bacteria (reviewed in (Dubrac *et al.*, 2008, Jordan *et al.*, 2008, Winkler & Hoch, 2008). Although the WalRK TCS shows distinctive features in each bacterial species, several unifying patterns have emerged about this TCS. The WalR response regulator is generally essential and required for growth in culture (Fabret & Hoch, 1998, Hancock & Perego, 2004, Kadioglu *et al.*, 2003, Martin *et al.*, 1999, Senadheera *et al.*,

[#]Dedicated to the memory of Professor Howard Gest (Indiana University Bloomington)

[*]Corresponding author: Department of Biology Indiana University Bloomington 1001 East Third Street - Jordan Hall 142 Bloomington, Indiana 47405 Phone: 812-856-1318 winklerm@indiana.edu.
[1]Contributed equally to this work

2005, Throup *et al.*, 2000, Wagner *et al.*, 2002), although bypass suppressors can be identified that uncouple regulon expression from WalR control (Delaune *et al.*, 2011, Ng *et al.*, 2003, Winkler & Hoch, 2008). WalR proteins are members of the PhoB family of response regulators and consist of phosphorylated receiver domains and winged-helix DNA-binding effector domains that contain characteristic structural features (see (Barbieri *et al.*, 2010, Bent *et al.*, 2004, Doi *et al.*, 2010, Okajima *et al.*, 2008)).

The core of all WalRK regulons consists of genes encoding peptidoglycan hydrolases involved in cell division (Bisicchia *et al.*, 2010, Bisicchia *et al.*, 2007, Dubrac *et al.*, 2007, Dubrac & Msadek, 2004, Liu & Burne, 2011, Ng et al., 2003, Ng *et al.*, 2005, Senadheera *et al.*, 2012). Other gene classes in the regulon vary among different bacteria and include genes that mediate wall teichoic acid biosynthesis, exopolysaccharide production, or virulence (Botella *et al.*, 2011, Duque *et al.*, 2011, Liu *et al.*, 2006, Mohedano *et al.*, 2005, Ng et al., 2005, Senadheera et al., 2005). With the exception of *pcsB* homologues in some *Streptococcus* species (Barendt *et al.*, 2009, Ng *et al.*, 2004, Ng et al., 2003), the essentiality of WalR is caused by regulation of multiple genes (Bisicchia et al., 2007, Delaune et al., 2011, Dubrac et al., 2008). Mutations that activate WalR function lead to the formation of wall-less L-form cells (Dominguez-Cuevas *et al.*, 2012), and other amino acid changes in WalR result in vancomycin-intermediate resistance of *Staphylococcus aureus* (VISA) laboratory strains and clinical isolates (Howden *et al.*, 2011, Shoji *et al.*, 2011) .

In contrast to WalR, WalK sensor kinases are divided into two distinct classes (Fukushima *et al.*, 2008, Ng & Winkler, 2004, Turck & Bierbaum, 2012). WalK homologues of *Bacillus*, *Staphylococcus*, *Enterococcus*, and most other species contain two transmembrane domains flanking an extracytoplasmic domain (Fukushima et al., 2008, Szurmant *et al.*, 2007b), which is the typical arrangement for many histidine kinases (see (Gao & Stock, 2009)). The transmembrane domains of *Bacillus subtilis* $WalK_{Bsu}$ interact with the membrane domains of the auxiliary WalHI (YycHI) proteins away from the division septum to negatively regulate phosphorylation levels of $WalR_{Bsu}$ (Fukushima *et al.*, 2011, Szurmant *et al.*, 2008, Szurmant *et al.*, 2007a). In contrast, $WalK_{Spn}$ from *Streptococcus pneumoniae* (pneumococcus), which exemplifies the other class, contains a single transmembrane domain connected to an extracellular peptide of only 12 amino acids, and *S. pneumoniae* lacks homologues of WalHI (Fig. 1) (Ng & Winkler, 2004). Another major difference between the two WalK classes is that members of the majority class, exemplified by $WalK_{Bsu}$, are generally essential for bacterial growth in culture, whereas *Streptococcal* WalK sensor kinases are dispensable, although their absence may impair growth (Fabret & Hoch, 1998, Ng et al., 2003, Senadheera et al., 2012).

The cytoplasmic domains of both classes of WalK sensors are similar and contain a HAMP (linker) domain followed by a PAS (potential signal binding or protein interaction) domain, which precedes the DHp (dimerization/histidine phosphorylation) and catalytic CA (ATPase) domains, characteristic of sensor kinases (Fig. 1) (Gao & Stock, 2009, Henry & Crosson, 2011). In addition, both classes of WalRK TCS involve an auxiliary protein, called WalJ (YycJ), which is a predicted member of the metallo-β-lactamase superfamily (Ng & Winkler, 2004, Turck & Bierbaum, 2012, Winkler & Hoch, 2008). Although its enzymatic function is unknown, accumulated data suggests links among WalJ, WalRK TCS function, and peptidoglycan metabolism that if perturbed, disrupt accurate coordination of cell division and DNA replication (Biller et al., 2011, Ng et al., 2003).

Cell wall damage by antibiotics is believed to be a signal that induces formation of WalR~P (Dubrac et al., 2008), although the mechanisms of signal transduction by WalRK and their auxiliary proteins remain largely unknown. WalK is randomly distributed in the membrane of dividing *S. pneumoniae* cells (Wayne *et al.*, 2010), in contrast to the septal location of

WalK$_{Bsu}$ in dividing *B. subtilis* cells (Fukushima et al., 2011). Changing the conserved, phosphorylated Asp52 residue of pneumococcal WalR to Asn, Gln, or Ala is not tolerated, implying that WalR~P formation is required for *pcsB* expression (Ng et al., 2003). Even the Asp52Glu change, which can mimic aspartyl phosphate, is barely tolerated, except in Δ*walK* mutants, suggesting additional interactions between WalK and WalR (Ng et al., 2003). Titration experiments indicated that WalR is present in excess in exponentially growing *S. pneumoniae* (Ng et al., 2003). Consistent with this expectation, WalR is an abundant protein present in ≈6,000 monomers per cell, which is a ≈13-fold molar excess over WalK dimer amount (Wayne et al., 2010).

Recently, we reported that the WalK sensor kinase of *S. pneumoniae* exhibits a strong phosphatase activity that mediates dephosphorylation of WalR~P in biochemical reactions (Gutu *et al.*, 2010, Huynh & Stewart, 2011). Optimal WalK phosphatase activity in reactions depended on its PAS domain (Gutu et al., 2010). In this study, we examine the roles of the WalK autokinase and phosphatase activities in setting WalRK regulon expression and WalR~P amount in exponentially growing *S. pneumoniae* cells. To this end, we identified an amino acid change in WalK that specifically reduces its phosphatase activity, and we modified the Phos-tag SDS-PAGE method (Barbieri & Stock, 2008) for use in *S. pneumoniae.* Our results support the conclusions that WalK phosphatase is the default activity in exponentially growing cells and that WalK prevents phosphorylation of WalR by non-cognate sensor kinases. Yet, we show that crosstalk phosphorylation of WalR is partly responsible for the viability of pneumococcal *walK* mutants. This work also demonstrates the utility of the Phos-tag SDS-PAGE method to determine response regulator phosphorylation levels in bacterial cells and a way to deal with a potential limitation of this method.

Results

WalK^{T222A} is defective in phosphatase activity, but not in other WalK activities

To understand more about the physiological roles of WalK phosphatase activity in *S. pneumoniae*, we needed to identify a phosphatase-deficient mutant of WalK that retained nearly normal autokinase and phosphoryltransferase activities. Huynh and Stewart recently proposed a reaction mechanism for the phosphatase activity mediated by transmitter domains of HisKA-family sensor kinases (Huynh *et al.*, 2010, Huynh & Stewart, 2011). Based on this model and on other previous studies of phosphatase deficient mutants of sensor kinases (Capra *et al.*, 2010, Dutta *et al.*, 2000, Hsing & Silhavy, 1997, Zhu *et al.*, 2000), we expressed and purified 13 mutant WalK proteins with amino acid changes in the DHp domain near the phosphorylated His218 residue (Fig. S1). The V216G, S217D, P223A, P223S, R221D, or T222D (Fig. S2) or T222R (Gutu et al., 2010) amino acid changes severely diminished autokinase activity and were not studied further.

Combined autokinase-phosphoryltransferase-phosphatase assays were performed to screen for decreased phosphatase activity of the remaining WalK mutant proteins (Fig. 2 and S3) (Gutu et al., 2010). In combined assays, little WalR~P accumulated in Mg^{2+} buffer because of the WalK phosphatase activity (Gutu et al., 2010). More WalR~P accumulated in Ca^{2+} than Mg^{2+} buffer because of the strong dependence of the phosphatase activity on Mg^{2+} ion (Gutu et al., 2010, Huynh & Stewart, 2011, Zhu et al., 2000). WalK with the T225A, S217A, or R221K amino acid changes (Fig. S3C, S3D, and S3H) showed similar low-level accumulation of WalR~P as wild-type WalK^{+} in Mg^{2+} buffer and were not ostensibly defective in phosphatase or other WalK activities. The T222A, R221A, R221S, or T222Y amino acid changes in WalK resulted in increased WalR~P accumulation in Mg^{2+} buffer (Fig. 2 and S3B, S3F, and S3G), characteristic of a defect in WalK phosphatase activity

(Gutu et al., 2010). Of these, WalK^{T222A} showed the strongest effect (Fig. 2) and was characterized further.

The increase in WalR~P accumulation in combined assays containing WalK^{T222A} could be the result of increased autokinase or phosphoryltransferase activity or decreased phosphatase activity. Michaelis-Menton kinetic analysis of the autokinase reaction showed that WalK^{T222A} has a similar K_m (ATP) to that of wild-type WalK^{+}, and a slightly lower k_{cat} (Fig. S4), which would not account for greater accumulation of WalR~P in combined assays (Fig. 2). We estimated the catalytic efficiency of the phosphoryltransfer reaction containing WalK^{T222A} or WalK^{+} by determining the half-life of WalK~P after WalR addition (Fig. S5) (see (Gutu et al., 2010)). The catalytic efficiency of phosphoryltransfer to WalR was greater in Mg^{2+} buffer than Ca^{2+} buffer as we reported before (Fig. S5) (Gutu et al., 2010). However, in both Mg^{2+} and Ca^{2+} buffers, the kinetic preference of phosphoryltransfer from wild-type WalK^{+}~P was slightly greater than from WalK^{T222A}~P (Fig. S5). The lower efficiency of phosphoryltransfer from WalK^{T222A}~P again would not account for the increase in WalR~P formation in the combined assays (Fig. 2). Finally, we assayed the phosphatase activity of WalK^{T222A} using a direct HPLC-based assay (Fig. S6 and S7) (Gutu et al., 2010). The phosphatase activity mediated by WalK^{T222A} was at least 13-fold lower than that of WalK^{+}. We conclude that greatly reduced phosphatase activity accounts for the accumulation of WalR~P in combined assays containing WalK^{T222A} (Fig. 2), which has comparatively minor defects in its autokinase and phosphoryltransferase activities. This conclusion was confirmed by determination of the cellular amounts of WalR~P in a *walK*^{T222A} mutant as described below.

WalK autokinase activity is required for optimal pneumococcal growth in statically aerated cultures

Four isogenic mutants were studied to learn more about the roles of the WalK autokinase and phosphatase activities in growth of encapsulated *S. pneumoniae* strain D39 (Table S1). The Δ*walK*, *walK*^{H218A}, and *walK*$^{\Delta PAS}$ mutants were reported previously and contain an in-frame markerless deletion of the central region of the *walK* gene, a nucleotide substitution that changes the phosphorylated His218 to Ala in WalK, and an internal in-frame deletion that removes the PAS domain of WalK, respectively (Gutu et al., 2010). In biochemical assays using truncated WalK derivatives, WalK^{H218A} has no autokinase activity and shows ≈12-fold less phosphatase activity than wild-type WalK^{+} (Gutu et al., 2010). WalK$^{\Delta PAS}$ has ≈12-fold less phosphatase activity, but is kinetically defective in that its K_m (ATP) in the autokinase reaction is increased by ≈6-fold compared to that of wild-type WalK^{+}, while its k_{cat} is similar (Gutu et al., 2010). However, the increased K_m (ATP) (≈300 μM) of WalK$^{\Delta PAS}$ remains below the total ATP concentration (≈2,000 μM) in exponentially growing *S. pneumoniae* D39 cells (Ramos-Montanez, et al., 2010). The *walK*^{T222A} mutant was constructed for this study (see above).

Repeated growth determinations showed that the autokinase-deficient Δ*walK* and *walK*^{H218A} mutants consistently grew slightly (≈14%) slower and reached a lower (≈45%) final OD_{620} (growth yield) than the *walK*$^{+}$ parent strain in cultures grown statically in BHI broth in an atmosphere of 5% CO_2 without additional aeration (Fig. 3A and S8A) (Gutu et al., 2010). In comparison, the *walK*$^{\Delta PAS}$ and *walK*^{T222A} phosphatase-deficient mutants grew at the same rate as the *walK*$^{+}$ parent strain, although the growth yield of the *walK*^{T222A} mutant was consistently slightly lower (≈15%) than that of the parent (Fig. 3A and S8A). The decreased growth yield of the *walK*^{H218A} mutant compared to the *walK*$^{+}$ and *walK*^{T222A} strains could not be attributed to cell death or premature autolysis during exponential phase or the transition to stationary phase (Fig. S8 and S9).

Importantly, the *walK*^{H218A} point mutation should not be polar on downstream *walJ* expression, and similar amounts of WalK$^{\Delta PAS}$, WalK^{H218A}, and WalK^{+} were detected by Western blotting in cultures during exponential growth (Fig. S8C). The Δ*walK* mutation, which retained 60 bp from each end of the gene, was also not polar on downstream transcription of *walJ* as determined by microarray analyses (Table 1). Notably, inactivation of *walK* caused decreased relative transcript amounts confined predominantly to members of the WalRK regulon, including *spd_0104* (−3.1 fold; LysM protein), *spd_0703* (−1.9 fold; putative SEDS protein), *spd_1874* (−4.4; putative *N*-acetylmuramidase), and *pcsB* (−2.6 fold; putative peptidoglycan hydrolase) (Barendt *et al.*, 2011, Ng et al., 2005, Sham *et al.*, 2011).

WalK^{T222A} increases WalRK regulon expression and cellular WalR~P amount

QRT-PCR assays confirmed the microarray results (Table 1) by showing that the relative transcript amounts of WalRK regulon genes *spd_1874* and *pcsB* dropped by 5- and 3-fold in the Δ*walK* and *walK*^{H218A} mutants, respectively, compared to the *walK*$^{+}$ parent (Fig. 4A and S10A). Control experiments indicated that the drop in the relative amount of *spd_1874* transcript was complemented by ectopic expression of the *walK*$^{+}$ gene (Fig. S10B). In subsequent experiments, we used relative amounts of *spd_1874* transcript from QRT-PCR assays as a read out of regulon expression, because *spd_1874* responds the most strongly to the WalRK TCS (Table 1) (Ng et al., 2005). We conclude that WalK autokinase activity and phosphoryltransfer to WalR are necessary to maintain normal WalRK regulon expression in exponentially growing cells.

The WalK PAS domain is required for optimal phosphatase activity in biochemical reactions, but WalK$^{\Delta PAS}$ also has a kinetic defect in the autokinase activity (see above) (Gutu et al., 2010). The *walK*$^{\Delta PAS}$ mutant showed ≈30% less WalRK regulon expression compared to the *walK*$^{+}$ parent (Fig. 4A). In contrast, the *walK*^{T222A} phosphatase mutant showed a large (7-fold) increase in WalRK regulon expression (Fig. 4A), consistent with an increased cellular amount of WalR~P.

To understand these regulation patterns further, we determined the cellular amounts of WalR and WalR~P in these mutants (Fig. 4B and 5) by a modification of the Phos-tag SDS-PAGE method reported by Barbieri and Stock (Barbieri & Stock, 2008). The acid extraction procedure used in (Barbieri & Stock, 2008) gave poor protein yields in Gram-positive *S. pneumoniae.* We overcame this problem by optimizing and validating a rapid extraction procedure for quantitative determinations of pneumococcal WalR and WalR~P amounts by Phos-tag SDS-PAGE (Experimental procedures; Supplemental Information; Fig. 5, S11, and S12). In these experiments, the total amount of WalR detected by Western blotting remained constant in each strain tested (data not shown).

Three main results were obtained from these experiments. First, the percentage of WalR~P clearly increases in the *walK*$^{\Delta PAS}$ and *walK*^{T222A} mutants compared to the other strains (Fig. 4B and 5A). Remarkably, the percentage of WalR~P is ≈90% in the *walK*^{T222A} mutant. As a control, heating samples from the *walK*^{T222A} mutant converted all WalR~P to WalR, consistent with the heat-lability of aspartyl-phosphate bonds (Fig. 5A, right). Second, there is a correlation between WalRK regulon expression and percentage of WalR~P in mutants (Δ*walK*; *walK*$^{\Delta PAS}$, *walK*^{H218A}, *walK*^{T222A}, Δ*walK* Δ*pnpR*, and Δ*walK* Δ*pnpRS*) defective in WalK phosphatase activity (Fig. 4, 5, and 6 (see next section)). This correlation can be visualized by fitting values on a non-linear exponential curve (not shown). Third, unlike the mutants, the correlation between regulon expression and percentage of WalR~P breaks down in the WalK^{+} parent strain, which contained a barely detectable amount of WalR~P (Fig. 4 and 5A). The most likely explanation for this lack of correlation is loss of WalR~P during cell lysis of strains with active WalK phosphatase activity (see Discussion).

Together, these results support the conclusion that WalK phosphatase is strongly active in exponentially growing pneumococcal cells and that mutational inactivation of WalK phosphatase activity results in high levels of WalR~P, accompanied by a large increase in WalRK regulon expression.

The idea that WalK phosphatase can predominate over autokinase activity was further supported by *in vitro* experiments. In cells, most response regulators are present in large molar excess over their cognate sensor kinases (see (Goulian, 2010)). It was proposed that for certain TCSs, the importance of phosphatase activity was overestimated, because sensor kinases were present in molar excess over their cognate response regulators in coupled biochemical reactions (Kenney, 2010). Our experiments do not support this idea for the $WalRK_{Spn}$ TCS. In exponentially growing strain D39, ≈7-fold more WalR monomer is present than WalK monomer (i.e., 13-fold more WalR monomer than WalK dimer) (Wayne et al., 2010). At comparable molar ratios, WalR~P did not accumulate in coupled reactions containing $WalK^{+}$ in Mg^{2+} buffer (Fig. 7 and S13). In contrast, WalR~P did accumulate in reactions containing $WalK^{+}$ and Ca^{2+} buffer or in reactions containing phosphatase-deficient $WalK^{T222A}$ (Fig. 6). We conclude that WalK functions primarily as a phosphatase in biochemical reactions, consistent with the strong WalK phosphatase activity detected in unstressed growing cells (Fig. 4 and 5).

WalK phosphatase activity limits crosstalk in exponentially growing cells

The amount of WalR~P in the Δ*walK* and $walK^{H218A}$ mutants was close to the limit of detection of this method (Fig. 4B and 5A). The residual WalR~P detected in Δ*walK* and $walK^{H218A}$ mutants likely reflects crosstalk. One source of crosstalk is phosphorylation by non-cognate histidine kinases in the absence of WalK function. Alignment of other HisKA-family sensor kinases revealed that the DHp recognition helix of WalK (HK02) has a similar amino acid sequence to that of the PnpS (HK04), HK06, VncS (HK10), CiaH (HK05), and HK08 senor kinases (Fig. S14). We expressed and purified soluble truncated derivatives of these other 5 histidine kinases to test whether they could phosphorylate non-cognate WalR (Table S3; Fig. S14 and S15). In coupled reactions containing cognate WalK~P, WalR~P was detected rapidly within 1 min, despite WalK phosphatase activity (Fig. S7). In contrast, a low level of crosstalk phosphorylation of WalR to WalR~P was detected for non-cognate PnpS~P, HK08~P, and CiaH~P after long incubation times of >10 min (Fig. S15B, S15C, and S15D). No WalR~P was detected for non-cognate VncS~P and HK06~P (Fig. S15E and S15F), which phosphorylated their cognate response regulators, VncR and RR06 (Fig. S15G and S15H). We conclude that crosstalk between PnpS~P, HK08~P, and CiaH~P and non-cognate WalR requires long incubation times in biochemical reactions and is not kinetically favored compared to cognate WalK~P (see (Laub *et al.*, 2007, Laub & Goulian, 2007)).

Of the pneumococcal sensor kinases, the DHp recognition domains of WalK and PnpS are the most closely matched (Fig. S14); therefore, PnpS was a likely candidate for crosstalk to WalR in cells. The pneumococcal PnpRS TCS likely regulates phosphate uptake in *S. pneumoniae* (Moreno-Letelier *et al.*, 2011, Novak *et al.*, 1999). Moreover, in *B. subtilis*, crosstalk was detected between the $PhoR_{Bsu}$ histidine kinase, which is the homologue of $PnpS_{Spn}$, and $WalR_{Bsu}$ (Bisicchia et al., 2010, Botella et al., 2011, Howell *et al.*, 2006). Indeed, we detected significant phosphorylation of WalR in a Δ*walK* Δ*pnpR* mutant, which lacks WalK and the PnpR response regulator (Fig. 5B and 7B). WalR~P accumulation in the Δ*walK* Δ*pnpR* mutant led to ≈4-fold greater WalRK regulon expression than in the Δ*walK* mutant (Fig. 7A) and corrected the growth defect of the Δ*walK* mutant (Fig. 3B).

The increase in percentage of cellular WalR~P was abrogated in a Δ*walK* Δ*pnpRS* mutant, indicating that PnpS phosphorylated WalR in the absence of WalK in the Δ*walK* Δ*pnpR* mutant (Fig. 5B and 7B). WalRK regulon expression was reduced in the Δ*walK* Δ*pnpRS*

mutant compared to the Δ*walK* mutant (Fig. 7A), showing that the PnpS sensor kinase contributed to the crosstalk that allowed growth of the Δ*walK* mutant under these conditions. Finally, for the three *walK*$^+$ strains with corresponding alleles of *pnpRS* (*walK*$^+$ *pnpRS*$^+$; *walK*$^+$ Δ*pnpR*; and *walK*$^+$ Δ*pnpRS*), there was again a lack of correlation between WalRK regulon expression and the percentage of WalR~P (Fig. 7A and 7B). WalRK regulon expression was maintained around the wild-type level, whereas apparent WalR~P amounts were low compared to the Δ*walK* Δ*pnpR* mutant (Fig. 7A and 7B). As discussed below, maintenance of wild-type levels of regulon expression in the *walK*$^+$ strains is consistent with a role of WalK phosphatase in preventing crosstalk from PnpS and other non-cognate sensor kinases during exponential growth.

Discussion

WalK phosphatase is the default activity in biochemical reactions and exponentially growing pneumococcal cells

In this study, we further analyzed the contributions of the WalK autokinase and phosphatase activities in setting WalRK regulon expression and WalR~P amounts in non-stressed, exponentially growing cells of *S. pneumoniae*. We also examined the role of crosstalk as the basis for the non-essentiality of pneumococcal WalK. To carry out these studies, we identified the WalK^{T222A} mutant sensor kinase that is deficient for WalK mediated dephosphorylation of WalR~P, but proficient in autokinase or phosphoryltransferase activities (Fig. 2, S4-S7). We also optimized the Phos-tag SDS-PAGE method to quantitate WalR phosphorylation levels in the *walK*^{T222A} and other *walK* mutants (Fig. 5, S11, and S12). We identified WalK^{T222A} by a biochemical screen based on amino acids predicted to be involved in the WalK-mediated phosphatase reaction (Results; Fig. S1). According to a recent model proposed by Huynh and Steward (Huynh et al., 2010, Huynh & Stewart, 2011), Thr222 of WalK$_{Spn}$ should coordinate a water molecule for nucleophilic hydrolysis of the aspartyl-phosphate group of WalR~P. Our finding that the T222A (and to a lesser extent the Thr222Y (Fig. S3G)) substitution results in a phosphatase-deficient, autokinase-proficient WalK supports this role for Thr222. However, other changes made at Thr222 (e.g., T222D and T222R) strongly decreased WalK autokinase activity (Fig. S3) (Gutu et al., 2010), possibly by perturbing the structure of the DHp domain.

Our combined data support the idea that the WalK phosphatase is the default activity in biochemical reactions and in unstressed pneumococcal cells growing exponentially. In coupled biochemical reactions containing physiological ratios of WalR to WalK, WalK phosphatase activity predominated over autokinase activity and prevented accumulation of WalR~P (Fig. 6). WalR~P only accumulated to appreciable amounts in reactions containing phosphatase-deficient WalK^{T222A} instead of WalK$^+$. Most importantly, the *walK*^{T222A} mutation greatly increased WalRK regulon expression by ≈7-fold (Fig. 4A) and increased the percentage of WalR~P to ≈90% in exponentially growing cells (Fig. 4B). Constitutive overexpression of the WalRK regulon in the *walK*^{T222A} mutant did not decrease growth rate or significantly alter yield (Fig. 3A and S8A) or strongly affect cell morphology or viability (Fig. S8B and S9). Most members of the WalRK regulon likely function as murein hydrolases, whose activities are allosterically regulated by cell division proteins (Sham et al., 2011, Sham *et al.*, 2012, Uehara & Bernhardt, 2011, Yang *et al.*, 2011). Therefore, overexpression alone of these proteins may not be deleterious to growing cells. For example, overexpressed PcsB would likely be secreted into the growth medium, because the amount of PcsB bound to the cell surface is set by the amount of its interaction partner, the FtsX integral membrane protein (Sham et al., 2011). Taken together, these results support the idea that WalK phosphatase activity plays a major role in setting the amount of WalR~P and the level of WalRK regulon expression in exponentially growing *S. pneumoniae* cells. If the

WalK phosphatase activity is ablated, WalR becomes nearly completely phosphorylated to WalR~P, even in unstressed exponentially growing cells.

WalRK regulon expression correlates with cellular WalR~P amount in mutants deficient in WalK phosphatase activity, but not in *walK*$^+$ cells

WalRK regulon expression was correlated with percentage of WalR~P for *walK* mutants deficient in phosphatase activity, but not for phosphatase-proficient *walK*$^+$ strains (see Results). The simplest and most likely explanation for this non-correlation is that WalR~P was lost during cell lysis of *walK*$^+$ strains due to WalK phosphatase activity. More complicated explanations, such as function of unphosphorylated WalR, require additional assumptions to account for other trends in the data and are difficult to reconcile with the requirement for the aspartate residue that becomes phosphorylated in WalR (Introduction). Initial tests limited loss of WalR~P from *walK*$^+$ bacteria to the lysis step. Mixing equal densities of *walK*$^+$ (7% WalR~P) and *walK*^{T222A} (90% WalR~P) bacteria before extraction resulted in ≈50% WalR~P, indicating that loss of WalR~P was not occurring in the extracts after cell disruption (data not shown). Longer chilling of cultures before centrifugation and addition of commercially available phosphatase inhibitor cocktails (from Pierce or Roche) did not increase the proportion of WalR~P in *walK*$^+$ strains (data not shown). Additional extraction protocols need to be tested to address this potential limitation of the Phos-tag SDS-PAGE method. Nevertheless, we can use the correlation in the phosphatase-deficient strains and the regulon expression levels in *walK*$^+$ strains to calculate relative WalR~P amounts. Based on this correction, ≈26% WalR~P is present in the non-stressed, exponentially growing *walK*$^+$ strains (dotted lines in Fig. 4 and 7).

The assumption that relative WalR~P amount is underestimated in phosphatase-proficient *walK*$^+$ strains allows interpretation of other trends in these data. The *walK*$^{\Delta PAS}$ mutant showed modestly decreased (≈30%) WalRK regulon expression compared to the *walK*$^+$ strain (Fig. 4A). This decreased regulon expression, which was insufficient to affect growth (Fig. 3A), implied that the autokinase kinetic defect of WalK$^{\Delta PAS}$ (see Results) may have decreased WalR~P amount in cells. Consistent with this interpretation, the ≈16% WalR~P recovered from the *walK*$^{\Delta PAS}$ mutant is less than the ≈26% WalR~P estimated for the *walK*$^+$ strain (Fig. 4B). Moreover, the fact that we recovered increased WalR~P (≈2.5-fold) from the *walK*$^{\Delta PAS}$ mutant compared to the *walK*$^+$ parent (Fig. 4B) supports the idea that WalK$^{\Delta PAS}$ is deficient in phosphatase activity in cells as well as in biochemical reactions (Gutu et al., 2010). Another important implication of this interpretation comes from the increased recovery of WalR~P from antibiotic treated *walK*$^+$ bacteria (Fig. S11C) (K. Kazmierczak, in preparation). Recovery of a substantial amount of WalR~P from a *walK*$^+$ strain implies that the WalK phosphatase activity is somehow blocked during cell wall stress, perhaps by interaction with a ligand or another protein.

WalK autokinase activity is required for normal pneumococcal growth and cell morphology

The absence of WalK autophosphorylation in the *walK*^{H218A} or Δ*walK* mutant caused moderate growth defects that did not reflect a severe drop in cell viability (Fig. 3, S8, and S9). These phenotypes contrast with the severe drop in cell viability reported recently for Δ*walK*$_{Smu}$ mutants of *S. mutans* (Senadheera et al., 2012), which is distantly related to *S. pneumoniae* (Kawamura *et al.*, 1995, Sultana *et al.*, 1998). This difference in growth phenotypes may reflect the composition of the WalRK regulons in these two bacterial species. In *S. mutans*, inactivation of *walK*$_{Smu}$ led to changes in relative transcription of genes from many functional classes, including bacteriocin and competence genes (Senadheera et al., 2012). In contrast, we show here that inactivation of *walK*$_{Spn}$ decreased expression of a small number of genes that primarily mediates peptidoglycan hydrolysis

(Table 1). Expression of this same limited set of genes was increased when *pcsB* was underexpressed, suggesting feedback control (Fig. 1B) (Barendt et al., 2009). Likewise, expression of this core set of murein hydrolase genes was increased or decreased when $walR_{Spn}$ expression was increased or decreased, respectively (Mohedano et al., 2005, Ng et al., 2003, Ng et al., 2005). Lack of $WalK_{Spn}$ autokinase activity resulted in ≈3-fold less *pcsB* gene transcription (Table 1; Fig. S10). Previous work shows that this degree of *pcsB* underexpression is sufficient to account for the slight decrease in growth rate, markedly lower growth yield, and moderate defects in cell morphology of the Δ*walK* and $walK^{H218A}$ mutants (Barendt et al., 2009).

These combined observations suggest an attractive model that will be tested in future experiments (Fig. 1B and S16). In exponentially growing *S. pneumoniae*, the PAS domain regulates WalK phosphatase activity to set the basal WalR~P amount and WalRK regulon expression level. Cell wall damage or limitation of PcsB amount induces a ligand or another protein to bind to the PAS domain and turn off WalK phosphatase activity, thereby increasing relative WalR~P amount and WalRK regulon expression. It has not been determined whether the PAS domain of $WalK_{Bsu}$ might play a similar role in *B. subtilis*, but the PAS domain of $WalK_{Bsu}$ does have an additional function compared to its counterpart in $WalK_{Spn}$. The PAS domain of $WalK_{Bsu}$ interacts with the divisome and directs the localization of $WalK_{Bsu}$ to the septum of dividing *B. subtilis* cells (Fukushima et al., 2011). In contrast, $WalK_{Spn}$ is randomly distributed in the membrane of dividing *S. pneumoniae* cells (Wayne et al., 2010).

Crosstalk accounts for the non-essentiality of *walK* mutations in *S. pneumoniae*

Δ*walK* and $walK^{H218A}$ mutants, which are deficient in both autokinase and phosphatase activities (see Results), contained ≈8% WalR~P (Fig. 4B, Fig. 5, Fig. 7B) and were moderately impaired in growth (Fig. 3 and S8). The Δ*walK* Δ*pnpR* mutant strikingly exhibited crosstalk phosphorylation of WalR by PnpS; the percentage of WalR~P increased from 8% to 24% (Fig. 5B and 7B), WalRK regulon expression increased by ≈4-fold (Fig. 7A), and wild-type growth was restored (Fig. 3B) compared to the Δ*walK* mutant. These increases disappeared in a Δ*walK* Δ*pnpRS* mutant demonstrating that crosstalk in the Δ*walK* Δ*pnpR* mutant depended on PnpS function (Fig. 7). Furthermore, the 2-fold drop in WalRK regulon expression, decrease in relative WalR~P amount, and impaired growth of the Δ*walK* Δ*pnpRS* mutant compared to the Δ*walK* mutant (Fig. 3B and 7B) shows that crosstalk to WalR by PnpS contributes to the viability of *walK* mutants. In comparison, a comparable analysis indicated that acetyl phosphate, which is plentiful (≈3 mM) in *S. pneumoniae,* contributed negligibly (≈20%) to maintaining WalRK regulon expression in a Δ*walK* mutant (Ramos-Montanez *et al.*, 2010). Presumably, the barely detectable, residual (<3%) amount of WalR~P left in the Δ*walK* Δ*pnpRS* mutant is provided by CiaH and HK08, which phosphorylated WalR inefficiently *in vitro* (Fig. S15C and S15D). It remains to be determined whether a Δ*walK* Δ*pnpRS* Δ*ciaH* Δ*hk08* mutant is viable in the absence of constitutive PcsB expression (see (Ng et al., 2003, Ng et al., 2005)). Since the WalR response regulator is abundant (≈6,000 monomers per cell), it is also possible that unphosphorylated WalR may activate sufficient expression of the WalRK regulon (see (Bourret, 2010, Gao *et al.*, 2007, Gao & Stock, 2010)) to allow some level of growth in the absence of WalR phosphorylation by crosstalk.

In contrast, no level of crosstalk seems to occur in $walK^{+}$ *S. pneumoniae* growing exponentially. Expression of the WalRK regulon was the same in the $walK^{+}$ $pnpRS^{+}$ (parent), $walK^{+}$ Δ*pnpR*, and $walK^{+}$ Δ*pnpRS* strains (Fig. 7A). As discussed above, the low recovery of WalR~P from these $walK^{+}$ strains likely reflects WalK phosphatase activity during cell lysis. Following the correction described above, the percentage of WalR~P is ≈26% in each of these strains (dashed line, Fig. 7B). Thus, $WalK^{+}$ function sets the level of

WalRK regulon expression and presumably WalR~P amount. Notably, no crosstalk was detected in the *walK*$^+$ Δ*pnpR* mutant, despite the capacity of PnpS to phosphorylate WalR in the Δ*walK* Δ*pnpR* mutant (Fig. 7B). In *B. subtilis,* the PhoR$_{Bsu}$ sensor kinase, which responds to phosphate limitation, phosphorylates WalR$_{Bsu}$ in *walK*$^+$ strains during phosphate limitation to provide a form of physiological cross regulation that links cell wall maintenance to the phosphate stress response (Botella et al., 2011, Howell *et al.*, 2003, Howell et al., 2006). It remains to be determined whether certain combinations of stress conditions, such as cell wall damage and phosphate limitation, elicit similar cross regulation in *S. pneumoniae*. Paradoxically, both PhoR$_{Bsu}$ of *B. subtilis* and PnpS$_{Spn}$ of *S. pneumoniae* seem to have the capacity to phosphorylate their WalR homologues in Δ*walK* mutants. Yet, this crosstalk only occurs in *S. pneumoniae walK* mutants (Fig. 7A), and *walK* mutations are lethal to *B. subtilis* (Fabret & Hoch, 1998). Perhaps the additional function of WalK$_{Bsu}$ in cell division described above (Fukushima et al., 2011), which is lacking in *S. pneumoniae* (Wayne et al., 2010), accounts for this difference in the essentiality of WalK$_{Bsu}$ and WalK$_{Spn}$.

Experimental procedures

Pneumococcus strains and growth conditions

Bacterial strains used in this study are listed in Supplemental Table S1. *S. pneumoniae* cultures were grown statically in Brain-Heart Infusion broth (BHI; Becton-Dickinson BD) or on plates containing Trypticase Soy Agar II modified (BD) and 5% (v/v) defibrinated sheep blood (Remel) (TSAII BA) at 37°C in an atmosphere of 5% CO_2. Growth was monitored directly by determining OD_{620} using a Spectronic 20 Genesys spectrophotometer. For overnight cultures, strains were inoculated from frozen stocks into 5 ml of BHI broth in 17-mm-diameter polystyrene plastic tubes, serially diluted over five tubes, and grown for 11 to 13 h. Cultures at OD_{620} ≈0.1 to 0.3 were adjusted to OD_{620} ≈0.1 with fresh BHI and diluted 1/100 into BHI broth to start final cultures, which lacked antibiotics. For strain constructions, antibiotics were present at concentrations indicated in Table S1.

Viability determinations by live-dead staining

Overnight and final cultures were grown as described above. 500 μL of culture were removed at the indicated stages of growth. Cells were collected by centrifugation at 16,100 × *g* for 2 min at 25°C, suspended in 50 μl of fresh BHI broth with gentle pipetting, and stained without fixation by adding 2 μL of a 1:1 (v/v) mixture of Syto-9 and propidium iodide (LIVE/DEAD *Bac*Light Bacterial Viability Kit, Molecular Probes) for 5 min in the dark at 25°C. Stained bacteria were examined using a Nikon E-400 epifluorescence phase-contrast microscope with FITC and Texas Red bandpass filters, and phase-contrast and fluorescent images were captured using a cooled digital SPOT camera as described before (Barendt et al., 2009). At least 100 and as many as 1,300 bacteria from 2 to 7 microscopic fields were examined for each time point. The experiment was performed 3 times with similar results.

Strain constructions

Oligonucleotide primers used in strain constructions are listed in Table S2. *walK* mutants in *S. pneumoniae* were constructed by the Janus method of allele replacement used previously (Table S1) (Gutu et al., 2010, Ramos-Montanez *et al.*, 2008, Sung *et al.*, 2001, Wayne et al., 2010). *walK* mutants were described previously (Gutu et al., 2010), except for w*alK*^{T222A}, which was constructed by crossing a w*alK*^{T222A} linear amplicon into strain IU1885 (Table S1). Mutations in the *pnpRS* locus were constructed by replacing the *pnpR* or *pnpRS* reading frames with an Erm^R antibiotic cassette in strains IU1896 and IU1781 (Table S1).

RNA extraction

Overnight cultures were grown as described above and inoculated into 30 ml BHI broth cultures contained in 50 ml conical centrifuge tubes to a starting OD_{620} ≈0.001. At OD_{620} ≈0.2, RNA was extracted from 4 ml of exponentially growing cultures by a hot lysis-acid phenol extraction followed by purification using an RNAeasy minikit (Qiagen) and on-column DNaseI treatment as described previously (Barendt et al., 2009, Kazmierczak *et al.*, 2009). For QRT-PCR assays, 5 μg of total RNA was further digested with DNase using a DNA-free kit (Ambion).

Microarray analysis

Microarray analyses were performed as described in (Barendt et al., 2009) to compare relative transcript amounts of strains IU1896 (Δ*walK*) and IU1781 (*walK*$^{+}$). Total RNA was prepared as described above from 10 ml cultures. Microarrays were purchased from Ocimum Biosolutions. Synthesis, labeling, hybridization, scanning, normalization, and analysis using the Cyber-T web interface were performed as described previously (Barendt et al., 2009). Fold changes and Bayesian *P*-values were based on 3 independent biological replicates, including a dye swap. Intensity and expression ratio data for all transcripts are deposited in the GEO database, accession number GSE19752.

Construction of recombinant protein-expression plasmids

Plasmids used in this study are listed in Table S1. Genomic DNA used to construct plasmids was isolated from *S. pneumoniae* laboratory strain R6, which has the same DNA sequences of the cloned genes as strain D39 (Lanie *et al.*, 2007). PCR amplicons generated with the primers in Table S2 were cloned into the *Bam*HI and *Bsa*I sites of plasmid pSumo (LifeSensors, Inc.) to generate protein expression plasmids. Plasmids were transformed into *E. coli* strain DH5α (Bioline) for storage and into strain Rosetta 2(DE3) (Novagen) or Tuner (EMD) for protein expression and purification (Tables S1 and S3). Deletion and point mutations in cloned histidine kinases were generated by fusion PCR as described previously (Gutu et al., 2010) using PCR primers listed in Table S2.

Protein expression and purification

Recombinant (N)-His-WalR, other response regulators, and truncated histidine kinases (Table S3) were purified as described previously (Gutu et al., 2010), with the following modifications. *E. coli* strains were grown with shaking at 37°C to OD_{620} ≈0.4 to 0.6 in Difco LB broth (BD) supplemented with antibiotics required for plasmid maintenance (see Table S1). Protein expression was induced by addition of 0.2 mM isopropyl-1-thio-β-D-galactopyranoside (IPTG; Calbiochem), followed by incubation at 16°C overnight with shaking (220 rpm). Cells were collected by centrifugation at 8,000 x g at 4°C for 30 min and stored at −80°C.

Cell pellets were suspended in cold buffer A (20 mM $NaPO_4$, 0.5 M NaCl, 40 mM imidazole, pH 7.4) supplemented with 50 μl per g of cell pellet of Protease Inhibitor set III (Calbiochem). Cells were lysed by two passes through a chilled French pressure cell (20,000 lb in^{-2}) and insoluble material was removed by two centrifugations at 12,000 x *g* for 20 min at 4°C. Lysates were filtered through a 0.2-μm pore-size membrane (Pall) before loading onto a HiTrap Chelating HP column (GE Healthcare) charged with 0.1 M $NiSO_4$ (Sigma) according to the manufacturer's instructions and equilibrated with buffer A. Filtrates were loaded at a flow rate of 1 ml per min at 4°C. Loaded columns were washed with cold buffer A for 15 min and proteins were eluted by imidazole gradients as described previously (Gutu et al., 2010). Fractions containing purified recombinant protein were pooled, concentrated, and exchanged into the optimized storage buffers listed in Table S3. Purified protein

samples were centrifuged at 100,000 x *g* for 15 min at 4°C to remove any remaining insoluble material and distributed to several tubes for storage at −80 °C. The concentration of purified proteins was determined by using the DC protein assay kit (Bio-Rad) with bovine serum albumin (Sigma Fraction V) as the standard. The purity of the protein samples was >95% based on Coomassie-stained gels (data not shown).

Autophosphorylation of WalK mutant proteins

(N)-Sumo-ΔN35-WalK proteins (2.0 μM) containing amino acid changes in the DHp recognition helix (Fig. S1) were equilibrated in Mg^{2+} reaction buffer (50 mM Tris-HCl (pH 7.6), 200 mM KCl, 5.0 mM $MgCl_2$) for 10 min at 25°C. Autophosphorylation reactions were started by the addition of 100 μM of [γ-^{33}P]ATP (0.25 Ci/ mmol, Perkin-Elmer). Samples were removed at 10, 30, and 60 min, analyzed by SDS-PAGE, and quantified by phosphorimaging as described in (Gutu *et al.*, 2010).

Combined autophosphorylation-phosphoryltransfer-phosphatase assay

Combined assays were carried out as described previously (Gutu et al., 2010) with the following modifications. Purified truncated (N)-Sumo-ΔN35-WalK (final concn = 2.0 μM) or mutant derivatives of WalK containing amino acid substitutions (Fig. S1) were equilibrated in 100 μl of Mg^{2+} or Ca^{2+} reaction buffer (50 mM Tris-HCl (pH 7.6), 200 mM KCl, 5 mM $MgCl_2$ or 5 mM $CaCl_2$) for 10 min at 25 °C. Reducing agent was omitted from reaction buffers as described previously (Gutu et al., 2010). Autophosphorylation reactions were started by the addition of [γ-^{33}P] ATP (0.25 Ci/ mmol, Perkin-Elmer) to 100 μM. A 15 μl sample was removed after 30 min and mixed with an equal volume of 2X Laemmli sample buffer (Bio-Rad) containing 5% (vol/vol) β-mercaptoethanol (Sigma) to stop the reaction. At this time point (t=0), purified (N)-His-WalR was added (final concn = 6.6 μM) to the remaining reaction mixture to start the phosphoryltransfer reaction. Samples (15 μl) were removed 1, 10, and 30 min after WalR addition, stopped as above, and analyzed by 10% Tris-glycine SDS-PAGE as described in (Gutu et al., 2010). Dried gels were exposed to a storage phosphor screen (GE Healthcare) for at least 16 h and analyzed using ImageQuant and GraphPad Prism 5 software as described previously (Gutu et al., 2010).

Combined assays at different WalK:WalR ratios

Purified (N)-Sumo-ΔN35-WalK and (N)-His-WalR proteins were equilibrated in Mg^{2+} or Ca^{2+} reaction buffer for 10 min at 25°C. Reactions containing the following final protein concentrations: 6.0 μM WalK and 6.0 μM WalR (1:1); 1.0 μM WalK and 6.0 μM WalR (1:6); and 0.6 μM WalK and 6.0 μM WalR (1:10), were started by the addition of [γ-^{33}P] ATP (0.25 Ci/ mmol, Perkin-Elmer) to 100 μM. Samples were removed after 1, 30, and 60 min, analyzed by SDS-PAGE, and WalR~P amounts were quantitated by phosphorimaging as described above.

Determination of WalK^{T222A} autophosphorylation kinetic parameters

Autophosphorylation kinetic parameters were determined as described previously (Gutu et al., 2010) with the following modifications. Purified (N)-Sumo-ΔN35-WalK^{+} or (N)-Sumo-ΔN35-WalK^{T222A} protein (final concn = 1.0 μM) was equilibrated with Mg^{2+} reaction buffer (50 mM Tris-HCl (pH 7.6), 200 mM KCl, 5.0 mM $MgCl_2$) for 10 min at 25°C. Autophosphorylation reactions were started by addition of [γ-^{33}P] ATP (0.25 Ci/ mmol, Perkin-Elmer) to 6.0 μM, 12.5 μM, 50 μM, 100 μM, or 250 μM. Samples were removed after 15, 30, 45, and 60 sec, analyzed by SDS-PAGE, and quantified by phosphorimaging as described above. Quantitation of WalK~P in each lane and calculation of reaction rates and Michaelis-Menton kinetic parameters was performed as described in (Gutu et al., 2010).

Estimation of phosphoryltransfer efficiency between WalK~P constructs and WalR

The basis for the assay was described in (Gutu et al., 2010), and the assays were carried out with the following modifications. (N)-Sumo-ΔN35-WalK^{+} or (N)-Sumo-ΔN35-WalK^{T222A} protein (final concn = 3.0 μM) was equilibrated in Mg^{2+} or Ca^{2+} reaction buffer (50 mM Tris-HCl (pH 7.6), 200 mM KCl, 5.0 mM $MgCl_2$ or $CaCl_2$, 15% (vol/vol) glycerol) at 25°C for 5 min. Autophosphorylation reactions were started by the addition of [γ-^{33}P]ATP (0.25 Ci/ mmol, Perkin-Elmer) to 500 μM. After 20 min, excess ATP was removed from the reaction by using spin desalting columns (Pierce), and a sample of desalted protein was removed to determine the amount of WalK~P by SDS-PAGE. (N)-His-WalR (final concn = 0.5 μM or 1.0 μM) was added to the remaining desalted sample to initiate phosphoryltransfer. Samples were removed after 30, 60, 120, and 240 sec, analyzed by SDS-PAGE, and quantified by phosphorimaging. Phosphoryltransfer efficiency between WalK~P constructs and WalR was evaluated as described previously (Gutu et al., 2010).

Quantification of WalK^{T222A}-catalyzed dephosphorylation of WalR~P

Dephosphorylation activity of the (N)-Sumo-ΔN35-WalK^{T222A} protein was determined as reported previously (Gutu et al., 2010) with the following modifications. (N)-His-WalR (final concn = 6.0 μM) was phosphorylated with 40 mM acetyl phosphate (Sigma) in reaction buffer (50 mM Tris-HCl (pH 7.4), 200 mM KCl, 4.0 mM $MgCl_2$) at 37°C for 70 min. Excess acetyl phosphate was removed by using spin desalting columns (Thermo Scientific). Desalted WalR~P was incubated with 13.2 μM ADP (Sigma) in the presence or absence of 2.0 μM (N)-Sumo-ΔN35-WalK^{T222A} protein at 25°C. Samples were removed at time points ranging from 30 min to 240 min, mixed with eluent A (20% (vol/vol) acetonitrile and 0.1% (vol/vol) trifluoroacetic acid (EM Science) in water), and analyzed by reversed-phase HPLC using a Phenomenex Jupiter 300A C_4 column and a Shimadzu 10A HPLC system as described in (Gutu et al., 2010). The relative amount of WalR~P remaining at each time point was normalized to the starting amount of WalR~P, and half-lives were calculated as described previously (Gutu et al., 2010).

Autophosphorylation of other pneumococcal HisKA-family histidine kinases followed by phosphoryltransfer to WalR or cognate response regulators

Combined assays of autophosphorylation of truncated (N)-Sumo-ΔN206-PnpS, (N)-Sumo-ΔN58-HK08, (N)-Sumo-ΔN210-CiaH, (N)-Sumo-ΔN165-HK06, or (N)-Sumo-ΔN164-VncS and phosphoryltransfer to (N)-His-WalR were performed as described above for (N)-Sumo-ΔN35-WalK. Similar combined assays were performed with cognate pair (N)-Sumo-ΔN165-HK06 (final concn = 2.0 μM) and (N)-His-RR06 (final concn = 4.6 μM). Reactions containing (N)-Sumo-ΔN164-VncS (1.0 μM) were started by addition of [γ-^{32}P] ATP (0.5 Ci/mmol; Perkin-Elmer) to 250 μM. After 3 min (t=0), (N)-His-WalR or (N)-Sumo-VncR (final concn = 6.7 μM) was added, and samples were removed at the times indicated in Fig. S15.

QRT-PCR analysis

QRT-PCR analysis was performed as described in (Kazmierczak et al., 2009, Ramos-Montanez et al., 2008) with the following changes. First-strand cDNA was synthesized using a qScript Flex cDNA synthesis kit (Quanta Biosciences) according to the manufacturer's protocol. cDNA was diluted 6-fold and serially diluted in 5-fold steps 1 to 3 times more. QRT-PCR reactions contained 10 μL of 2× Brilliant III Ultra-Fast SYBR Green QPCR Master Mix (Agilent), 2.0 μL each of 2 μM QPCR primers (Table S2), 0.3 μL of a 1:500 dilution of ROX reference dye, and 6.0 μL of diluted cDNA. Data were collected using an MX3000P thermocycler (Stratagene) running the SYBR Green with dissociation curve program modified as per the manufacturer's recommendations and converted to the

Comparative Quantitation with calibrator experiment type for analysis (MxPro v. 3.0). Reactions were performed in duplicate using cDNA from at least two independent biological samples, and transcript amounts were normalized to *gyrA* RNA amount (Kazmierczak et al., 2009). Normalized transcript amounts were compared to that of the wild-type parent strain by performing pairwise unpaired two-tailed t tests (GraphPad Prism 5).

Phos-tag SDS-PAGE and quantitative Western blotting

The Phos-tag SDS-PAGE method was based on (Barbieri & Stock, 2008) with the additions and modifications described in Supplemental Information.

Validation of rapid extraction and Phos-tag SDS-PAGE

Several validation experiments were performed. Purified WalR and WalR~P phosphorylated by acetyl phosphate in biochemical reactions (see above) (Gutu et al., 2010) were resolved by 25 μM Phos-tag SDS-PAGE, although the resolution was not optimal (Fig. S11A and S11B). WalR~P and WalR were resolved and detected on Western blots of extracts prepared from exponentially growing cells (Fig. S11C). The percentage of WalR~P significantly increased in response to antibiotic stress conditions that stimulated WalRK regulon expression in the *walR*$^+$ *pcsB*$^+$ parent strain (Fig. S11C) (K. Kazmierczak, in preparation), and the WalR and WalR~P bands were not detected for a Δ*walR* P_c-*pcsB*$^+$ mutant, where the essential *pcsB* gene is expressed from a constitutive promoter (Fig. S11C) (Ng et al., 2003). Our anti-$WalR_{Spn}$ antibody cross reacted with a faint contaminant band in Western blots that sometimes interfered with quantitation of WalR~P amounts. Consequently, the Phos-tag acrylamide was increased to 50 μM and finally 75 μM, which moved WalR~P away from the contaminant band (Fig. 5 and S11C). In addition, we obtained the same results shown in Fig. 5 for strains expressing WalR-L-FLAG[3], which is detected with anti-FLAG antibody (see (Wayne et al., 2010)). Additional controls demonstrated that the WalR~P band was completely converted to WalR upon heating, as expected for the aspartyl-phosphate residue in WalR~P (Fig.5 and S12). Results from three control experiments argue against significant loss of WalR~P in extracts after cell disruption. We spiked purified WalR~P, which was phosphorylated in biochemical reactions, into suspensions of *walK*$^+$ parent cells right before they were disrupted. Since the amount of WalR~P recovered was extremely low in these cells (Fig. 4B and 5A), we were able to follow loss of the added WalR~P. We found minimal loss of WalR~P by Phos-tag SDS-PAGE (data not shown). Second, the amount of WalR~P is ≈90% in the *walK*^{T222A} strain (Fig. 4B and 5A), indicating minimal loss of cellular WalR~P in this modified procedure. Third, as mentioned in the text, mixing cultures of the *walK*$^+$ (WalR~P ≈7%) with *walK*^{T222A} (WalR~P ≈90%) mutants before the first centrifugation yielded ≈50% WalR~P on Phos-tag gels, consistent with minimal phosphatase activity in the extracts after cell disruption.

Supplementary Material

Refer to Web version on PubMed Central for supplementary material.

Acknowledgments

We thank Chris Sham and anonymous reviewers for detailed, critical comments about this work. We also thank Alina Gutu, Carl Bauer, Dan Kearns, David Kehoe, and Clay Fuqua for information and helpful discussions. K.J.W. was a predoctoral trainee on NIH Grant F31FM082090. This work was supported by NIAID grants AI060744 and AI095814 to M.E.W. and by funds from the Indiana University Bloomington METACyt Initiative, funded in part by a major grant from the Lilly Endowment, to M.E.W. The contents of this paper are solely the responsibility of the authors and do not necessarily represent official views of the funding agencies.

References

Barbieri CM, Mack TR, Robinson VL, Miller MT, Stock AM. Regulation of response regulator autophosphorylation through interdomain contacts. J Biol Chem. 2010; 285:32325–32335. [PubMed: 20702407]

Barbieri CM, Stock AM. Universally applicable methods for monitoring response regulator aspartate phosphorylation both in vitro and in vivo using Phos-tag-based reagents. Analyt Biochem. 2008; 376:73–82. [PubMed: 18328252]

Barendt SM, Land AD, Sham LT, Ng WL, Tsui HC, Arnold RJ, Winkler ME. Influences of capsule on the cell shape and chaining of wild-type and *pcsB* mutants of serotype 2 *Streptococcus pneumoniae*. J Bacteriol. 2009; 191:3024–3040. [PubMed: 19270090]

Barendt SM, Sham LT, Winkler ME. Characterization of mutants deficient in the L,D-carboxypeptidase (DacB) and WalRK (VicRK) regulon, involved in peptidoglycan maturation of *Streptococcus pneumoniae* serotype 2 strain D39. J Bacteriol. 2011; 193:2290–2300. [PubMed: 21378199]

Bent CJ, Isaacs NW, Mitchell TJ, Riboldi-Tunnicliffe A. Crystal structure of the response regulator 02 receiver domain, the essential YycF two-component system of *Streptococcus pneumoniae* in both complexed and native states. J Bacteriol. 2004; 186:2872–2879. [PubMed: 15090529]

Biller SJ, Wayne KJ, Winkler ME, Burkholder WF. The putative hydrolase YycJ (WalJ) affects the coordination of cell division with DNA replication in *Bacillus subtilis* and may play a conserved role in cell wall metabolism. J Bacteriol. 2011; 193:896–908. [PubMed: 21169496]

Bisicchia P, Lioliou E, Noone D, Salzberg LI, Botella E, Hubner S, Devine KM. Peptidoglycan metabolism is controlled by the WalRK (YycFG) and PhoPR two-component systems in phosphate-limited *Bacillus subtilis* cells. Mol Microbiol. 2010; 75:972–989. [PubMed: 20487291]

Bisicchia P, Noone D, Lioliou E, Howell A, Quigley S, Jensen T, Jarmer H, Devine KM. The essential YycFG two-component system controls cell wall metabolism in *Bacillus subtilis*. Mol Microbiol. 2007; 65:180–200. [PubMed: 17581128]

Botella E, Hubner S, Hokamp K, Hansen A, Bisicchia P, Noone D, Powell L, Salzberg LI, Devine KM. Cell envelope gene expression in phosphate-limited *Bacillus subtilis* cells. Microbiology. 2011; 157:2470–2484. [PubMed: 21636651]

Bourret RB. Receiver domain structure and function in response regulator proteins. Curr Opin Microbiol. 2010; 13:142–149. [PubMed: 20211578]

Capra EJ, Perchuk BS, Lubin EA, Ashenberg O, Skerker JM, Laub MT. Systematic dissection and trajectory-scanning mutagenesis of the molecular interface that ensures specificity of two-component signaling pathways. PLoS Genet. 2010; 6:e1001220. [PubMed: 21124821]

Delaune A, Poupel O, Mallet A, Coic YM, Msadek T, Dubrac S. Peptidoglycan crosslinking relaxation plays an important role in *Staphylococcus aureus* WalKR-dependent cell viability. PloS One. 2011; 6:e17054. [PubMed: 21386961]

Doi A, Okajima T, Gotoh Y, Tanizawa K, Utsumi R. X-ray crystal structure of the DNA-binding domain of response regulator WalR essential to the cell viability of *Staphylococcus aureus* and interaction with target DNA. Biosci Biotech Biochem. 2010; 74:1901–1907.

Dominguez-Cuevas P, Mercier R, Leaver M, Kawai Y, Errington J. The rod to L-form transition of *Bacillus subtilis* is limited by a requirement for the protoplast to escape from the cell wall sacculus. Mol Microbiol. 2012; 83:52–66. [PubMed: 22122227]

Dubrac S, Bisicchia P, Devine KM, Msadek T. A matter of life and death: cell wall homeostasis and the WalKR (YycGF) essential signal transduction pathway. Mol Microbiol. 2008; 70:1307–1322. [PubMed: 19019149]

Dubrac S, Boneca IG, Poupel O, Msadek T. New insights into the WalK/WalR (YycG/YycF) essential signal transduction pathway reveal a major role in controlling cell wall metabolism and biofilm formation in *Staphylococcus aureus*. J Bacteriol. 2007; 189:8257–8269. [PubMed: 17827301]

Dubrac S, Msadek T. Identification of genes controlled by the essential YycG/YycF two-component system of *Staphylococcus aureus*. J Bacteriol. 2004; 186:1175–1181. [PubMed: 14762013]

Duque C, Stipp RN, Wang B, Smith DJ, Hofling JF, Kuramitsu HK, Duncan MJ, Mattos-Graner RO. Downregulation of GbpB, a component of the VicRK regulon, affects biofilm formation and cell

surface characteristics of *Streptococcus mutans*. Infect Immun. 2011; 79:786–796. [PubMed: 21078847]

Dutta R, Yoshida T, Inouye M. The critical role of the conserved Thr247 residue in the functioning of the osmosensor EnvZ , a histidine kinase/phosphatase, in *Escherichia coli*. J Biol Chem. 2000; 275:38645–38653. [PubMed: 10973966]

Fabret C, Hoch JA. A two-component signal transduction system essential for growth of *Bacillus subtilis*: implications for anti-infective therapy. J Bacteriol. 1998; 180:6375–6383. [PubMed: 9829949]

Fukushima T, Furihata I, Emmins R, Daniel RA, Hoch JA, Szurmant H. A role for the essential YycG sensor histidine kinase in sensing cell division. Mol Microbiol. 2011; 79:503–522. [PubMed: 21219466]

Fukushima T, Szurmant H, Kim EJ, Perego M, Hoch JA. A sensor histidine kinase co-ordinates cell wall architecture with cell division in *Bacillus subtilis*. Mol Microbiol. 2008; 69:621–632. [PubMed: 18573169]

Gao R, Mack TR, Stock AM. Bacterial response regulators: versatile regulatory strategies from common domains. Trends Biochem Sci. 2007; 32:225–234. [PubMed: 17433693]

Gao R, Stock AM. Biological insights from structures of two-component proteins. Annu Rev Microbiol. 2009; 63:133–154. [PubMed: 19575571]

Gao R, Stock AM. Molecular strategies for phosphorylation-mediated regulation of response regulator activity. Curr Opin Microbiol. 2010; 13:160–167. [PubMed: 20080056]

Goulian M. Two-component signaling circuit structure and properties. Curr Opin Microbiol. 2010; 13:184–189. [PubMed: 20149717]

Gutu AD, Wayne KJ, Sham LT, Winkler ME. Kinetic characterization of the WalRK$_{Spn}$ (VicRK) two-component system of *Streptococcus pneumoniae*: dependence of WalK$_{Spn}$ (VicK) phosphatase activity on its PAS domain. J Bacteriol. 2010; 192:2346–2358. [PubMed: 20190050]

Hancock LE, Perego M. Systematic inactivation and phenotypic characterization of two-component signal transduction systems of *Enterococcus faecalis* V583. J Bacteriol. 2004; 186:7951–7958. [PubMed: 15547267]

Henry JT, Crosson S. Ligand-binding PAS domains in a genomic, cellular, and structural context. Annu Rev Microbiol. 2011; 65:261–286. [PubMed: 21663441]

Howden BP, McEvoy CR, Allen DL, Chua K, Gao W, Harrison PF, Bell J, Coombs G, Bennett-Wood V, Porter JL, Robins-Browne R, Davies JK, Seemann T, Stinear TP. Evolution of multidrug resistance during *Staphylococcus aureus* infection involves mutation of the essential two component regulator WalKR. PLoS Path. 2011; 7:e1002359.

Howell A, Dubrac S, Andersen KK, Noone D, Fert J, Msadek T, Devine K. Genes controlled by the essential YycG/YycF two-component system of *Bacillus subtilis* revealed through a novel hybrid regulator approach. Mol Microbiol. 2003; 49:1639–1655. [PubMed: 12950927]

Howell A, Dubrac S, Noone D, Varughese KI, Devine K. Interactions between the YycFG and PhoPR two-component systems in *Bacillus subtilis*: the PhoR kinase phosphorylates the non-cognate YycF response regulator upon phosphate limitation. Mol Microbiol. 2006; 59:1199–1215. [PubMed: 16430694]

Hsing W, Silhavy TJ. Function of conserved histidine-243 in phosphatase activity of EnvZ, the sensor for porin osmoregulation in *Escherichia coli*. J Bacteriol. 1997; 179:3729–3735. [PubMed: 9171423]

Huynh TN, Noriega CE, Stewart V. Conserved mechanism for sensor phosphatase control of two-component signaling revealed in the nitrate sensor NarX. Proc Nat Acad Sci USA. 2010; 107:21140–21145. [PubMed: 21078995]

Huynh TN, Stewart V. Negative control in two-component signal transduction by transmitter phosphatase activity. Mol Microbiol. 2011; 82:275–286. [PubMed: 21895797]

Jordan S, Hutchings MI, Mascher T. Cell envelope stress response in Gram-positive bacteria. FEMS Microbiol Rev. 2008; 32:107–146. [PubMed: 18173394]

Kadioglu A, Echenique J, Manco S, Trombe MC, Andrew PW. The MicAB two-component signaling system is involved in virulence of *Streptococcus pneumoniae*. Infect Immun. 2003; 71:6676–6679. [PubMed: 14573696]

Kawamura Y, Hou XG, Sultana F, Miura H, Ezaki T. Determination of 16S rRNA sequences of *Streptococcus mitis* and *Streptococcus gordonii* and phylogenetic relationships among members of the genus *Streptococcus*. Internat J System Bacteriol. 1995; 45:406–408.

Kazmierczak KM, Wayne KJ, Rechtsteiner A, Winkler ME. Roles of *rel* in stringent response, global regulation and virulence of serotype 2 *Streptococcus pneumoniae* D39. Mol Microbiol. 2009; 72:590–611. [PubMed: 19426208]

Kenney LJ. How important is the phosphatase activity of sensor kinases? Curr Opin Microbiol. 2010; 13:168–176. [PubMed: 20223700]

Lanie JA, Ng WL, Kazmierczak KM, Andrzejewski TM, Davidsen TM, Wayne KJ, Tettelin H, Glass JI, Winkler ME. Genome sequence of Avery's virulent serotype 2 strain D39 of *Streptococcus pneumoniae* and comparison with that of unencapsulated laboratory strain R6. J Bacteriol. 2007; 189:38–51. [PubMed: 17041037]

Laub MT, Biondi EG, Skerker JM. Phosphotransfer profiling: systematic mapping of two-component signal transduction pathways and phosphorelays. Meth Enzymol. 2007; 423:531–548. [PubMed: 17609150]

Laub MT, Goulian M. Specificity in two-component signal transduction pathways. Annu Rev Genet. 2007; 41:121–145. [PubMed: 18076326]

Liu M, Hanks TS, Zhang J, McClure MJ, Siemsen DW, Elser JL, Quinn MT, Lei B. Defects in *ex vivo* and *in vivo* growth and sensitivity to osmotic stress of group A *Streptococcus* caused by interruption of response regulator gene vicR. Microbiology. 2006; 152:967–978. [PubMed: 16549661]

Liu Y, Burne RA. The major autolysin of *Streptococcus gordonii* is subject to complex regulation and modulates stress tolerance, biofilm formation, and extracellular-DNA release. J Bacteriol. 2011; 193:2826–2837. [PubMed: 21478346]

Martin PK, Li T, Sun D, Biek DP, Schmid MB. Role in cell permeability of an essential two-component system in *Staphylococcus aureus*. J Bacteriol. 1999; 181:3666–3673. [PubMed: 10368139]

Mohedano ML, Overweg K, de la Fuente A, Reuter M, Altabe S, Mulholland F, de Mendoza D, Lopez P, Wells JM. Evidence that the essential response regulator YycF in *Streptococcus pneumoniae* modulates expression of fatty acid biosynthesis genes and alters membrane composition. J Bacteriol. 2005; 187:2357–2367. [PubMed: 15774879]

Moreno-Letelier A, Olmedo G, Eguiarte LE, Martinez-Castilla L, Souza V. Parallel evolution and horizontal gene transfer of the *pst* operon in Firmicutes from oligotrophic environments. Internat J Evol Biol. 2011; 2011:781642.

Ng WL, Kazmierczak KM, Winkler ME. Defective cell wall synthesis in *Streptococcus pneumoniae* R6 depleted for the essential PcsB putative murein hydrolase or the VicR (YycF) response regulator. Mol Microbiol. 2004; 53:1161–1175. [PubMed: 15306019]

Ng WL, Robertson GT, Kazmierczak KM, Zhao J, Gilmour R, Winkler ME. Constitutive expression of PcsB suppresses the requirement for the essential VicR (YycF) response regulator in *Streptococcus pneumoniae* R6. Mol Microbiol. 2003; 50:1647–1663. [PubMed: 14651645]

Ng WL, Tsui HC, Winkler ME. Regulation of the *pspA* virulence factor and essential *pcsB* murein biosynthetic genes by the phosphorylated VicR (YycF) response regulator in *Streptococcus pneumoniae*. J Bacteriol. 2005; 187:7444–7459. [PubMed: 16237028]

Ng WL, Winkler ME. Singular structures and operon organizations of essential two-component systems in species of *Streptococcus*. Microbiology. 2004; 150:3096–3098. [PubMed: 15470090]

Novak R, Cauwels A, Charpentier E, Tuomanen E. Identification of a *Streptococcus pneumoniae* gene locus encoding proteins of an ABC phosphate transporter and a two-component regulatory system. J Bacteriol. 1999; 181:1126–1133. [PubMed: 9973337]

Okajima T, Doi A, Okada A, Gotoh Y, Tanizawa K, Utsumi R. Response regulator YycF essential for bacterial growth: X-ray crystal structure of the DNA-binding domain and its PhoB-like DNA recognition motif. FEBS Lett. 2008; 582:3434–3438. [PubMed: 18789936]

Ramos-Montanez S, Kazmierczak KM, Hentchel KL, Winkler ME. Instability of *ackA* (acetate kinase) mutations and their effects on acetyl phosphate and ATP amounts in *Streptococcus pneumoniae* D39. J Bacteriol. 2010; 192:6390–6400. [PubMed: 20952579]

Ramos-Montanez S, Tsui HC, Wayne KJ, Morris JL, Peters LE, Zhang F, Kazmierczak KM, Sham LT, Winkler ME. Polymorphism and regulation of the *spxB* (pyruvate oxidase) virulence factor gene by a CBS-HotDog domain protein (SpxR) in serotype 2 *Streptococcus pneumoniae*. Mol Microbiol. 2008; 67:729–746. [PubMed: 18179423]

Senadheera DB, Cordova M, Ayala EA, Chavez de Paz LE, Singh K, Downey JS, Svensater G, Goodman SD, Cvitkovitch DG. Regulation of bacteriocin production and cell death by the VicRK signaling system in *Streptococcus mutans*. J Bacteriol. 2012; 194:1307–1316. [PubMed: 22228735]

Senadheera MD, Guggenheim B, Spatafora GA, Huang YC, Choi J, Hung DC, Treglown JS, Goodman SD, Ellen RP, Cvitkovitch DG. A VicRK signal transduction system in *Streptococcus mutans* affects *gtfBCD, gbpB*, and *ftf* expression, biofilm formation, and genetic competence development. J Bacteriol. 2005; 187:4064–4076. [PubMed: 15937169]

Sham LT, Barendt SM, Kopecky KE, Winkler ME. Essential PcsB putative peptidoglycan hydrolase interacts with the essential FtsX*Spn* cell division protein in *Streptococcus pneumoniae* D39. Proc Nat Acad Sci USA. 2011; 108:E1061–1069. [PubMed: 22006325]

Sham LT, Tsui HC, Land AD, Barendt SM, Winkler ME. Recent advances in pneumococcal peptidoglycan biosynthesis suggest new vaccine and antimicrobial targets. Curr Opin Microbiol. 2012; 15:194–203. [PubMed: 22280885]

Shoji M, Cui L, Iizuka R, Komoto A, Neoh HM, Watanabe Y, Hishinuma T, Hiramatsu K. *walK* and *clpP* mutations confer reduced vancomycin susceptibility in *Staphylococcus aureus*. Antimicrob Agent Chemother. 2011; 55:3870–3881.

Sultana F, Kawamura Y, Hou XG, Shu SE, Ezaki T. Determination of 23S rRNA sequences from members of the genus *Streptococcus* and characterization of genetically distinct organisms previously identified as members of the *Streptococcus anginosus* group. FEMS Microbiol Lett. 1998; 158:223–230. [PubMed: 9465395]

Sung CK, Li H, Claverys JP, Morrison DA. An *rpsL* cassette, Janus, for gene replacement through negative selection in *Streptococcus pneumoniae*. Appl Environ Microbiol. 2001; 67:5190–5196. [PubMed: 11679344]

Szurmant H, Bu L, Brooks CL 3rd, Hoch JA. An essential sensor histidine kinase controlled by transmembrane helix interactions with its auxiliary proteins. Proc Natl Acad Sci USA. 2008; 105:5891–5896. [PubMed: 18408157]

Szurmant H, Mohan MA, Imus PM, Hoch JA. YycH and YycI interact to regulate the essential YycFG two-component system in *Bacillus subtilis*. J Bacteriol. 2007a; 189:3280–3289. [PubMed: 17307850]

Szurmant H, White RA, Hoch JA. Sensor complexes regulating two-component signal transduction. Curr Opin Struct Biol. 2007b; 17:706–715. [PubMed: 17913492]

Throup JP, Koretke KK, Bryant AP, Ingraham KA, Chalker AF, Ge Y, Marra A, Wallis NG, Brown JR, Holmes DJ, Rosenberg M, Burnham MK. A genomic analysis of two-component signal transduction in *Streptococcus pneumoniae*. Mol Microbiol. 2000; 35:566–576. [PubMed: 10672179]

Turck M, Bierbaum G. Purification and activity testing of the full-length YycFGHI proteins of *Staphylococcus aureus*. PloS One. 2012; 7:e30403. [PubMed: 22276191]

Uehara T, Bernhardt TG. More than just lysins: peptidoglycan hydrolases tailor the cell wall. Curr Opinion Microbiol. 2011; 14:698–703.

Wagner C, Saizieu Ad A, Schonfeld HJ, Kamber M, Lange R, Thompson CJ, Page MG. Genetic analysis and functional characterization of the *Streptococcus pneumoniae vic* operon. Infect Immun. 2002; 70:6121–6128. [PubMed: 12379689]

Wayne KJ, Sham LT, Tsui HC, Gutu AD, Barendt SM, Keen SK, Winkler ME. Localization and cellular amounts of the WalRKJ (VicRKX) two-component regulatory system proteins in serotype 2 *Streptococcus pneumoniae*. J Bacteriol. 2010; 192:4388–4394. [PubMed: 20622066]

Winkler ME, Hoch JA. Essentiality, bypass, and targeting of the YycFG (VicRK) two-component regulatory system in gram-positive bacteria. J Bacteriol. 2008; 190:2645–2648. [PubMed: 18245295]

Yang DC, Peters NT, Parzych KR, Uehara T, Markovski M, Bernhardt TG. An ATP-binding cassette transporter-like complex governs cell-wall hydrolysis at the bacterial cytokinetic ring. Proc Nat Acad Sci USA. 2011; 108:E1052–1060. [PubMed: 22006326]

Zhu Y, Qin L, Yoshida T, Inouye M. Phosphatase activity of histidine kinase EnvZ without kinase catalytic domain. Proc Nat Acad Sci USA. 2000; 97:7808–7813. [PubMed: 10884412]

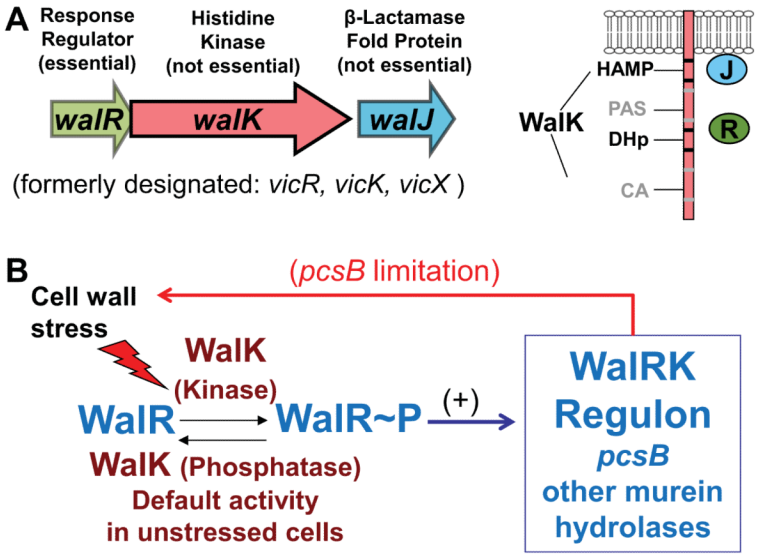

Fig. 1.

Genetic organization of the *walRKJ* operon in *S. pneumoniae* and model of WalRK$_{Spn}$ TCS function in exponentially growing and stressed cells. (A). The co-transcribed *walR* (response regulator), *walK* (histidine kinase/phosphatase) and *walJ* (auxiliary protein) genes are drawn to scale at left. *walR*, but not *walK* or *walJ,* is essential under normal growth conditions. Domains in one subunit of the WalK histidine kinase are shown at right, including the single membrane-spanning domain, the HAMP (linker) and PAS (signaling) domains, the DHp (dimerization/histidine phosphorylation) domain, and the CA (ATPase) catalytic domain. Both WalK and WalJ are membrane associated, whereas WalR is cytoplasmic (Wayne et al., 2010). (B) Model for WalRK signaling and gene regulation from this study. In exponentially growing cells, ≈26% WalR is phosphorylated, and functions to stimulate a basal level of WalRK regulon expression that maintains normal growth. In unstressed cells, WalK functions mainly as a phosphatase that sets the amount of WalR~P and limits crosstalk by non-cognate sensor kinases. In cells subjected to wall stresses or limitation of the *pcsB* regulon gene (signal arrow), the phosphatase activity of WalK is reduced, possibly by binding of a ligand or protein to the PAS domain of WalK, and the WalK autokinase/phosphoryltransferase reactions lead to increased amounts of WalR~P and regulon expression. See text for additional details.

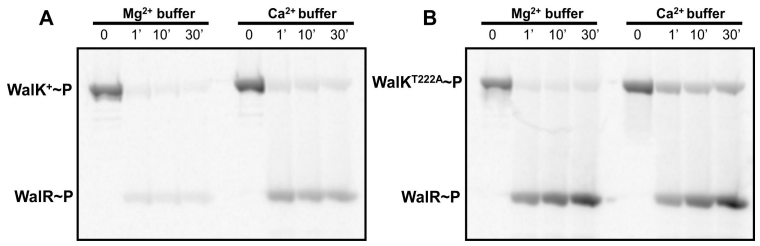

Fig. 2.

Combined assays of the autokinase, phosphoryltransfer, and phosphatase activities mediated by truncated $WalK^{+}$ or $WalK^{T222A}$. Reactions were performed at 25°C in reaction mixtures containing Mg^{2+} or Ca^{2+} buffer as described in Experimental procedures. Autophosphorylation reactions containing 2.0 μM of purified (A) (N)-Sumo-ΔN35-$WalK^{+}$ or (B) (N)-Sumo-ΔN35-$WalK^{T222A}$ protein proceeded for 30 min before (N)-His-WalR (final concn = 6.6 μM) was added without removal of ATP (t=0). The experiment was repeated >3 times, and representative phosphorimages of time courses are shown.

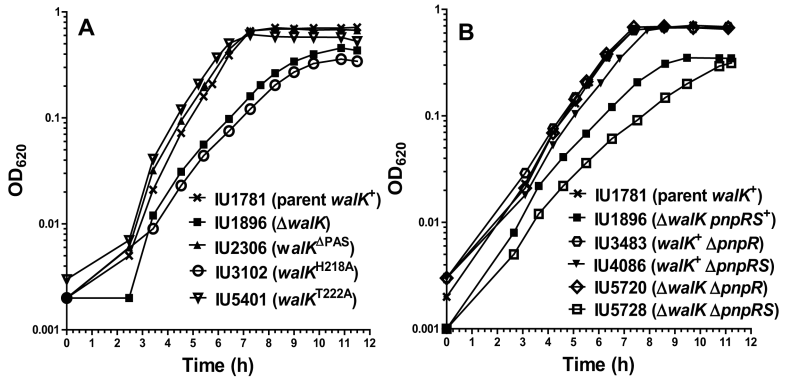

Fig. 3.

Representative growth curves of mutant strains used in this study. (A) *walK* mutant strains and (B) *walK pnpRS* mutant strains were grown in static BHI broth cultures at 37°C in an atmosphere of 5% CO_2 as described in Experimental procedures.

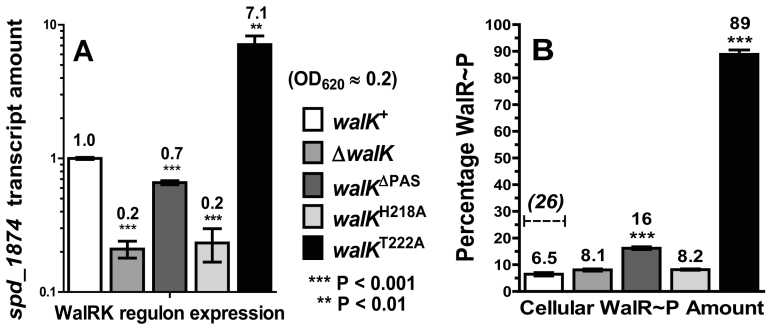

Fig. 4.

WalRK regulon expression in different *walK* mutant strains during exponential growth and corresponding cellular amounts of WalR~P. Strains were grown statically in BHI broth at 37°C in an atmosphere of 5% CO_2 to OD_{620} ≈ 0.2. RNA samples for QRT-PCR analysis and protein samples for Phos-tag SDS-PAGE were prepared and analyzed as described in Experimental procedures. *walK*$^+$ parent strain (IU1781); Δ*walK* (IU1896); *walK*$^{\Delta PAS}$ (IU2306); *walK*^{H218A} (IU3102); *walK*^{T222A} (IU5401). (A) Amounts of *spd_1874* transcript (a representative gene in the WalRK regulon) were normalized to that of *gyrA*. Transcript amounts are expressed relative to that of the *walK*$^+$ parent (≡ 1.0) and represent averages from duplicate samples from at least 2 independent experiments. Unpaired two-tailed t tests of relative transcript amounts compared to that of the *WalK*$^+$ parent were performed using GraphPad Prism 5 software. (B) Percentage of WalR~P compared to total WalR detected in extracts of *walK*$^+$ parent and *walK* mutant strains determined by Phos-tag SDS-PAGE and quantitative Western blotting with anti-$WalR_{Spn}$ antibody as described in Supplemental Information. The corrected amount of WalR~P in the *walK*$^+$ parent strain is indicated by the dotted line (see text). Averages are from 2 to 5 independent biological samples resolved on 50 and 75 μM Phos-tag acrylamide gels (see Fig. 5 and S12).

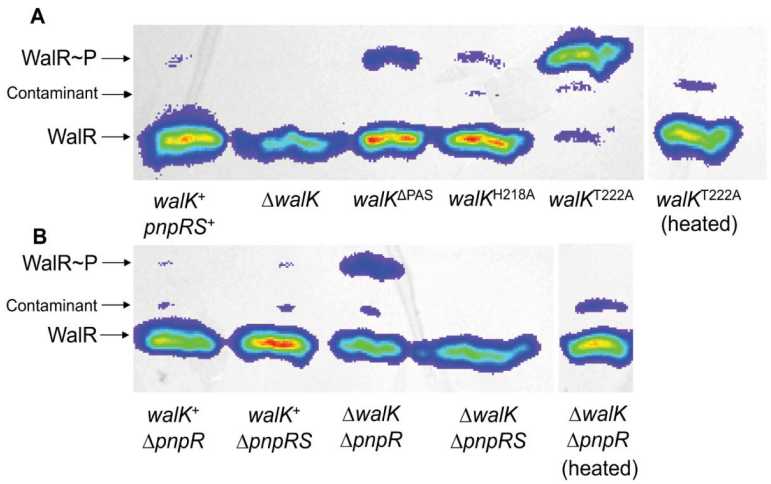

Fig. 5.

Representative Western blots of Phos-tag gels containing extracts of *walK* and *pnpRS* mutant strains grown exponentially in BHI broth. Growths, rapid preparation of protein extracts, 75 μM Phos-tag SDS-PAGE, and quantitative Western blotting with anti-WalR$_{Spn}$ antibody are described in Experimental procedures and Supplemental Information. The positions of unphosphorylated WalR, WalR~P, and a very faint contaminant band are indicated. (A) *walK*$^{+}$ parent strain (IU1781); Δ*walK* (IU1896); *walK*$^{\Delta PAS}$ (IU2306); *walK*^{H218A} (IU3102); *walK*^{T222A} (IU5401); and control heated sample of *walK*^{T222A} (IU5401) showing heat lability of WalR~P. (B) *walK*$^{+}$ Δ*pnpR* (IU3483); *walK*$^{+}$ Δ*pnpRS* (IU4086); Δ*walK* Δ*pnpR* (IU5720); Δ*walK* Δ*pnpRS* (IU5728); and control heated sample of Δ*walK* Δ*pnpR* (IU5720). Additional heated controls for extracts of other strains are shown in Fig. S12. The faint contaminant band was at the limit of detection and still present in extracts of a Δ*walR* P$_{c}$-*pcsB*$^{+}$ strain (EL1472), which lacks WalR and WalR~P (see Fig S11).

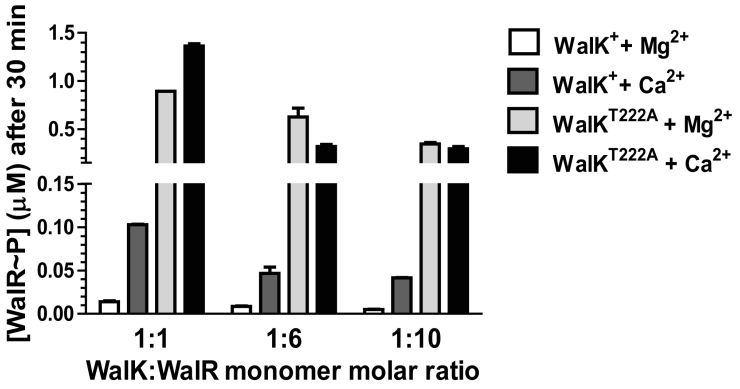

Fig. 6.

Dephosphorylation of WalR~P by WalK and WalK^{T222A} in combined assays containing physiologically relevant molar ratios of WalK sensor kinase to WalR response regulator (1:6.7) (Wayne et al., 2010). Combined assays were performed in buffers containing Mg^{2+} or Ca^{2+} ion as described in Experimental procedures, and amounts of WalR~P remaining after 30 min of incubation are shown. Similar trends were observed after 1 min and 60 min incubations (Fig. S13). Means with standard errors are indicated from 3 independent experiments.

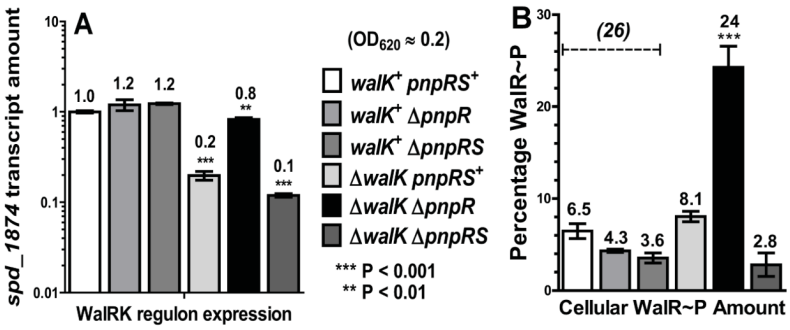

Fig. 7.

WalRK regulon expression in *walK* and *pnpRS* mutant strains during exponential growth and corresponding cellular amounts of WalR~P. Strains were grown statically in BHI broth at 37°C in an atmosphere of 5% CO_2 to $OD_{620} \approx 0.2$. RNA samples for QRT-PCR analysis and protein samples for Phos-tag SDS-PAGE were prepared and analyzed as described in Experimental procedures and Supplemental Information. *walK*$^+$ *pnpRS*$^+$ parent strain (IU1781); *walK*$^+$ Δ*pnpR* (IU3483); *walK*$^+$ Δ*pnpRS* (IU4086); Δ*walK* (IU1896); Δ*walK* Δ*pnpR* (IU5720); Δ*walK* Δ*pnpRS* (IU5728). (A) Amounts of *spd_1874* transcript were normalized to that of *gyrA*. Transcript amounts are expressed relative to that of the *walK*$^+$ parent (≡ 1.0) and represent averages from duplicate samples from at least 2 independent experiments. Unpaired two-tailed t tests of relative transcript amounts compared to that of the *walK*$^+$ parent were performed using GraphPad Prism 5 software. (B) Percentage of WalR~P compared to total WalR detected in extracts of *walK*$^+$ parent and *walK* and *pnpRS* mutant strains determined by Phos-tag SDS-PAGE and quantitative Western blotting with anti-$WalR_{Spn}$ antibody as described in Supplemental Information. The corrected amount of WalR~P in the *walK*$^+$ parent strain is indicated by the dotted line (see text). Averages are from 2 to 5 independent biological samples resolved on 50 and 75 μM Pho-tag acrylamide gels (see Fig. 5 and S12). The *walK*$^+$ *pnpRS*$^+$ and Δ*walK pnpRS*$^+$ data are from Fig. 4.

Table 1

Changes in relative transcript amounts in strain IU1896 (Δ*walK*) compared to IU1781 (*walK*$^+$) grown exponentially in BHI broth[a]

Gene tag	Gene description[b]	Fold changes	Bayesian *P* value
Decreased relative expression			
spd_0104	**LysM domain-containing protein**	**−3.1**	**8.6E-07**
spd_0391	Hypothetical protein	−1.9	2.5E-05
spd_0392	Hypothetical protein	−1.8	5.2E-05
spd_0447	*glnR*; transcriptional repressor of the glutamine synthetase gene	−1.7	4.3E-04
spd_0451	*hsdS*; type I restriction enzyme	−2.5	1.5E-06
spd_0703	**Hypothetical protein, putative SEDS protein**	**−1.9**	**3.0E-06**
spd_0853	***lytB*, N-acetylglucosaminidase**	**−1.6**	**6.9E-04**
spd_1824	Putative transmembrane protein with conserved FtsX superfamily domain	−1.6	1.4E-04
spd_1870	***pcp*-truncation; pyrrolidone carboxyl peptidase, truncation**	**−1.7**	**4.8E-05**
spd_1871	**Conserved hypothetical protein**	**−2.0**	**5.4E-06**
spd_1872	***marR*; transcriptional regulator - MarR family**	**−2.0**	**5.6E-05**
spd_1874	**LysM domain-containing protein, putative N-acetylmuramidase**	**−4.4**	**2.7E-07**
spd_2043	***pcsB*, putative peptidoglycan hydrolase**	**−2.6**	**1.6E-06**
Increased relative expression			
spd_0094	Hypothetical protein	1.6	4.7E-04
spd_0453	*hsdS*; type I site-specific deoxyribonuclease chain S	2.8	6.0E-07

[a] Strain construction, growth, and microarray analysis are described in Experimental procedures. RNA was prepared from exponential cultures grown to $OD_{620} \approx 0.2$. Fold changes and Bayesian *P*-values are based on 3 independent biological replicates, including a dye swap. Cutoffs for this table were 1.6-fold and $P<0.001$. A complete data set is deposited in GEO (accession GSE19752).

[b] Members of the WalRK$_{Spn}$ regulon are shown in bold type.